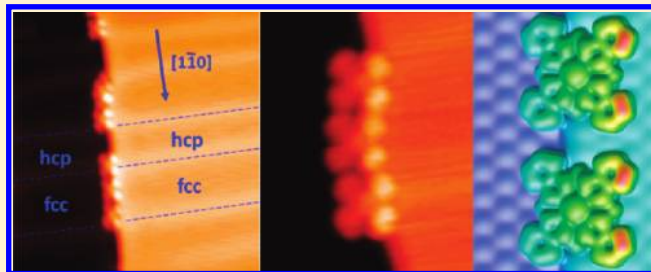


Site- and Configuration-Selective Anchoring of Iron–Phthalocyanine on the Step Edges of Au(111) Surface

Lizhi Zhang, Zhihai Cheng, Qing Huan, Xiaobo He, Xiao Lin, Li Gao, Zhitao Deng, Nan Jiang, Qi Liu, Shixuan Du,* Haiming Guo, and Hong-jun Gao*

Institute of Physics, Chinese Academy of Sciences, P.O. Box 603, Beijing 100190, People's Republic of China

ABSTRACT: Adsorption behavior of iron–phthalocyanine (FePc) at low submonolayer coverage on a reconstructed Au(111) single crystalline surface was investigated by a combination of low temperature scanning tunneling microscopy (STM) and density functional theory (DFT) calculations. A site- and orientation-selective adsorption was found at different temperatures and molecular coverages by means of STM. Further DFT calculations demonstrate that the energy difference between different adsorption configurations leads to the selectivity, and thus the formation of one-dimensional molecular chains on the monatomic step edges in the fcc surface reconstruction domains. The exact adsorption site and configuration of the FePc molecule as well as the simulated STM images are obtained on the basis of DFT calculations, which is in good agreement with experimental observations.



The exact adsorption site and configuration of the FePc molecule as well as the simulated STM images are obtained on the basis of DFT calculations, which is in good agreement with experimental observations.

1. INTRODUCTION

Organic functional nanostructures have attracted considerable attention in view of both the theoretical aspects of the physical properties of the organic–metal interface at the single molecule level and the potential application in molecular electronics.^{1–5} Therefore, many kinds of molecules have been investigated at various surfaces, including flat surfaces and periodically corrugated surfaces.⁶ The periodically corrugated surfaces have been suggested as an appropriate template for constructing ordered two-dimensional molecular structures, such as the high index vicinal surfaces,^{7,8} the Au(111) surface with a herringbone reconstruction pattern,^{9–11} and even the superstructures evolving from lattice mismatch.¹² Step edges, which are common and typical surface defects, may act as preferential adsorption sites and can be considered as an idea template for constructing one-dimensional (1D) structures, giving researchers a chance to investigate novel properties of 1D molecular structures.^{13–15}

Phthalocyanines (Pcs), metal–phthalocyanines (MPcs), and their derivatives have attracted considerable attention because of their extensive use in gas-sensing devices, photovoltaic applications, light-emitting diodes, solar and fuel cells, organic field effect transistors, and pigments and dyes.^{16–18} Consequently, investigations on the assembled structures of various MPcs have been reported, which are mainly focused on the monolayer structures.^{19–24} Recently, the single molecular rotor and the Kondo effect based on single MPc molecules have been investigated.^{25,26} In addition, it was reported that the cobalt–phthalocyanine has the self-organization phenomenon on the step edge of Au(788) surface.⁸ However, to our knowledge, few investigations on the mechanism of selective anchoring behavior of MPc molecules on a stepped metal substrate have been reported to date.

In this work, we successfully build 1D molecular nanostructures by site- and orientation-selective anchoring of FePc on monatomic steps of a reconstructed Au(111) substrate at different temperatures and different molecular coverages using a molecular-beam epitaxy (MBE), low temperature scanning tunneling microscopy (STM) combined system. It is found that the molecules prefer to adsorb at the step edges at both 5 and 77 K at low coverage. Increasing coverage results in adsorptions on terraces. Several possible adsorption configurations at the step edges and the terraces have been calculated based on density functional theory (DFT). We find that the experimental observed configuration at the step edge at 5 K has the highest adsorption energy among all of the configurations calculated, which suggests that it is a thermodynamically stable state. Moreover, the simulated STM image is in good agreement with the experimental observations. The adsorption energy of the configuration with one lobe rest on the step edge observed at 77 K is lower than that of the most stable one, which can be observed both at 5 and 77 K, but higher than that of the one adsorbed on the flat terrace. It implies that at 77 K, the molecules still prefer adsorbing on step edges rather than on flat terraces, which is also in good agreement with experimental results.

2. EXPERIMENTAL AND CALCULATION DETAILS

The experiments were performed with a low-temperature STM system (LT-STM, Omicron GmbH) equipped in an ultrahigh vacuum (UHV) chamber with a base pressure of 1×10^{-10} mbar.

Received: April 1, 2011

Revised: April 22, 2011

Published: May 11, 2011

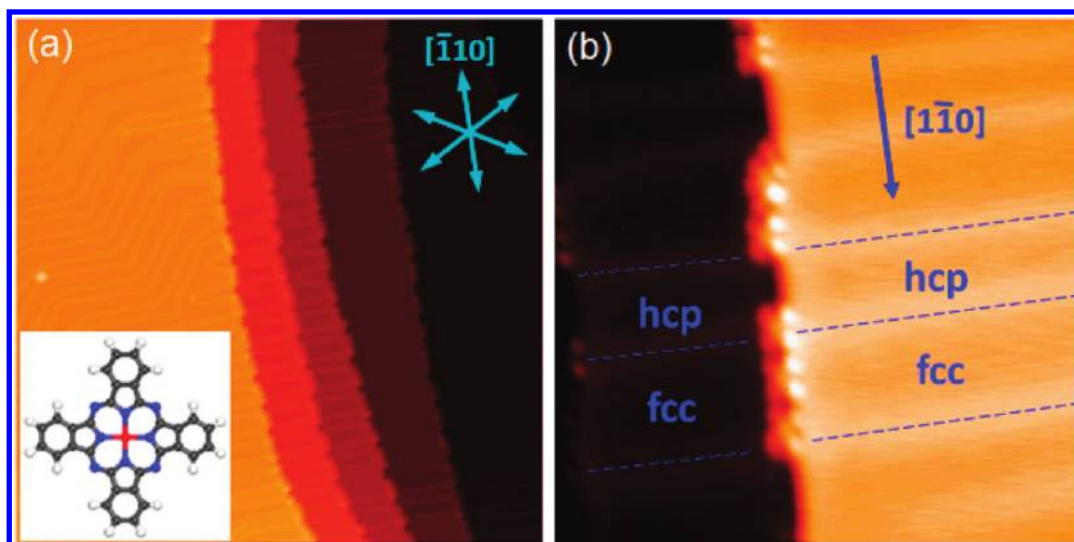


Figure 1. STM topography images of FePc adsorbed on Au(111) surface at very low coverage (~ 0.01 ML). (a) STM image ($150 \text{ nm} \times 150 \text{ nm}$, $U = -1.2 \text{ V}$, $I = 0.04 \text{ nA}$) of a large area with steps along the $[\bar{1}\bar{1}0]$ direction. The inset of (a) shows the schematic structural model of FePc. The set of three arrows in (a) indicates the closed-packed directions of the Au(111) substrate. (b) Close-up STM image ($25 \text{ nm} \times 25 \text{ nm}$, $U = -1.2 \text{ V}$, $I = 0.05 \text{ nA}$) of FePc molecules selectively decorating the step edges of a Au(111) surface. The FePc molecules decorate the step edges only within fcc surface reconstruction domains. The broken lines in (b) indicate the domain walls of the Au(111) herringbone reconstruction, which run perpendicular to the step edges.

The Au(111) surface was prepared by several cycles of Ar^+ ion sputtering, then annealing to 700 K, until a clean surface was confirmed by STM imaging. FePc (Aldrich, 98 + %) molecules were effectively purified using the temperature gradient sublimation method and immediately loaded into the sublimation cells. FePc molecules were thermally evaporated at 540 K onto the Au(111) surface, kept at room temperature, with MBE-LEED.^{27–29} One monolayer (ML) is defined as the amount of deposited FePc that entirely covers the substrate surface. The evaporation rate is about 0.025 ML/min. Subsequently, the sample was cooled to 5 K directly in the STM chamber. Electrochemically etched polycrystalline tungsten tips were used as STM tips, which were further cleaned by Ar^+ ion sputtering and annealing in UHV. All given voltages referred to the sample, and the images were taken in constant-current mode. All of the STM images were obtained at 5 K, except the indicated ones.

Our theoretical calculations were based on density-functional theory with the plane-wave basis sets, as implemented in the Vienna ab initio simulation package (VASP).^{30,31} The projector augmented wave (PAW) potentials were used to describe the core electrons and the generalized gradient approximation of Perdew, Burke, and Ernzerhof (PBE)³² for exchange and correlation. The periodic slab models included four and a half layers, one FePc molecule put on the side with step, and a vacuum layer of 15 Å. All of the atoms were fully relaxed except for the bottom two substrate layers until the net force on every atom was less than 0.02 eV/Å. In our calculation, the energy cutoff of the plane-wave basis sets was 400 eV, and a single Γ point is employed for Brillouin zone matrix integrations due to the numerical limitations.

3. RESULTS AND DISCUSSION

FePc, a typical planar MPc molecule, is composed of a flat phthalocyanine (Pc) skeleton with an iron atom completely in the central cavity, as schematically shown in the inset of Figure 1a.

Au(111) is a well-known substrate with $22 \times \sqrt{3}$ herringbone reconstruction.^{33–35} Two regions, the wide face-centered cubic (fcc) and the narrow hexagonal close-packed (hcp) stacking regions, are separated by discommensuration lines. Dashed blue lines indicate the discommensuration lines between the fcc and hcp stacking regions, running perpendicular to the step edges. After a very low coverage (~ 0.01 ML) of FePc molecules is deposited onto the Au(111) surface at room temperature, the terraces of the reconstructed Au(111) remain empty, and only the step edges are decorated with FePc molecules, as shown in Figure 1. The three arrows in Figure 1a represent the equivalent close-packed directions of the Au(111) surface. During room-temperature deposition, FePc molecules move quickly on the terraces and diffuse to their preferred adsorption sites at step edges. It should be noticed that only the step edges in fcc stacking region are covered by molecules at very low coverage and show a sawtoothed structure presented in Figure 1. This indicates that the FePc molecules decorate the step edges selectively. A close-up STM image of the Au(111) surface crossed by two decorated monatomic step edges along the $[\bar{1}\bar{1}0]$ direction is shown in Figure 1b. The STM images reveal that the step segments intersected by fcc domains (fcc step edges) are densely decorated with FePc molecules, forming rough evenly spaced one-dimensional (1D) molecular short chains, while the segments intersected by hcp domains (hcp step edges) are almost unoccupied by molecules. This strong preferential adsorption behavior at the step edges indicates that the adsorption site on the fcc step edge is more active than that on the hcp step edge for FePc molecules, which implies that the binding energy of FePc molecules on the fcc step edges is higher than that on the hcp step edges. This behavior is similar to that of the prototypical hexa-peri-hexabenzocoronene molecule on Au(111) surface,¹¹ which also decorates the fcc step edges selectively.

As the deposition coverage increases, the molecules adsorbed on both fcc and hcp step edges with two lobes resting on the upper terrace. After the step edges are all occupied, the molecules

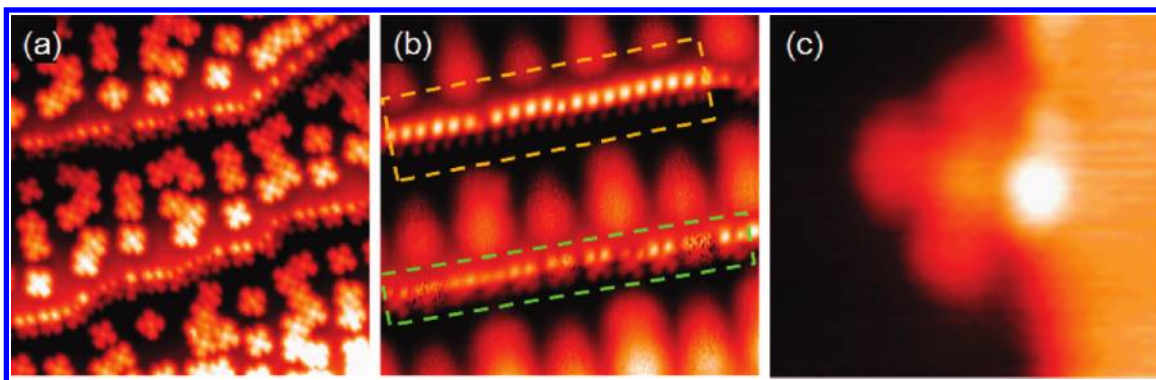


Figure 2. (a) STM image ($24 \text{ nm} \times 24 \text{ nm}$, $U = -1.5 \text{ V}$, $I = 0.05 \text{ nA}$) of FePc molecules decorating the step edges completely at a coverage of $\sim 0.6 \text{ ML}$. (b) STM image ($24 \text{ nm} \times 20 \text{ nm}$, $U = -1.2 \text{ V}$, $I = 0.05 \text{ nA}$) of FePc molecules decorating the step edges completely at the same coverage as (a), but taken at 77 K . (c) High-resolution STM image ($5 \text{ nm} \times 4 \text{ nm}$, $U = -1.5 \text{ V}$, $I = 0.05 \text{ nA}$) of FePc molecules adsorbing on a monatomic step edge with a configuration different from that above.

start decorating the terraces. Figure 2a shows the STM image with a coverage of $\sim 0.6 \text{ ML}$, in which both fcc and hcp step edges are completely decorated with FePc molecules, and molecules appear on the terraces as well. The STM images show that the FePc molecules on the hcp step edges have an adsorption configuration similar to those on the fcc step edges. The molecules on the step edges do not act as capturing nuclei for further growth from steps during the cooling process, indicating a weak interaction between the molecules on the terraces and that on the step edges.

Figure 2b shows the STM image of the same sample as in Figure 2a, but taken at 77 K . The noise patterns on the terraces are attributed to the fast diffusion of FePc molecules on the reconstructed Au(111) terraces.^{36,37} At the same time, most of the molecules on the step edges could be resolved in the STM image with two lobes resting on the upper terrace, which are indicated by the green dashed rectangle in Figure 2b. Yet we find that the configuration of molecules indicated by the yellow dashed rectangle could not be resolved. We attribute this phenomenon to the thermal vibration of a metastable state.

A new adsorption configuration of FePc molecules on the step edges is also observed at 77 K , with only one lobe resting on the upper terrace, as shown in Figure 2c. This special packing feature was found only at 77 K and at the high molecule coverage during our STM experiments. So we can conclude that the formation of this special packing feature is related to the influence of the thermal kinetic energy of the FePc molecule at a higher temperature of 77 K . The special adsorption configuration can be excited by the thermal energy at 77 K .

The FePc molecules are recognized as a four-lobed “cross” structure with a central protrusion both on the step edges and on terraces, as shown in Figure 3a and b. STM images of molecules adsorbed on monatomic step edges show that two lobes rest on the upper terrace, while the other two lobes rest on the lower terrace with the centered iron ion clearly resolved. It can be clearly seen that the apparent shape of the molecule has been reduced to D_{2h} symmetry, unlike its D_{4h} symmetric molecular structure. The dash lines in Figure 3c show the line profiles of Figure 3a. The lobe on the upper terrace has a maximum height of $\sim 3.45 \text{ \AA}$ above the lower Au(111) terrace, while that on the lower terrace gradually decreases from the step edges, with a height of $\sim 2.25 \text{ \AA}$ (black dash line in Figure 3c). The height of the central iron ion is $\sim 2.63 \text{ \AA}$, which is $\sim 0.82 \text{ \AA}$ lower than the upper lobes and $\sim 0.38 \text{ \AA}$ higher than the lower lobes. An STM

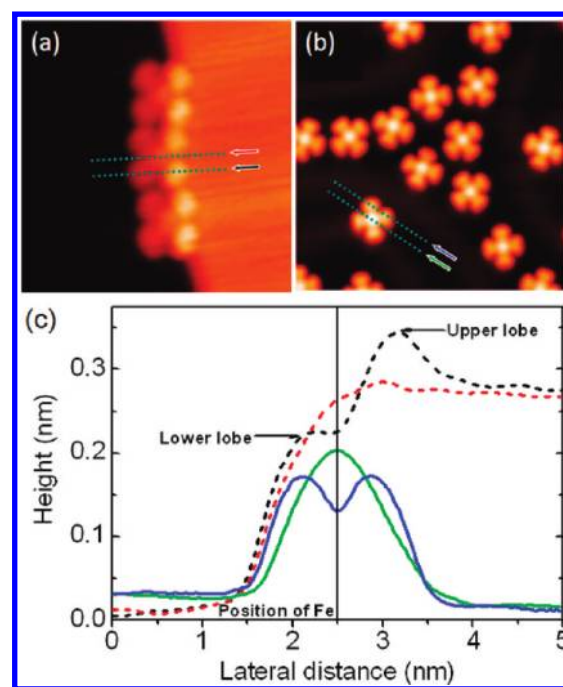


Figure 3. (a) High-resolution STM image ($7 \text{ nm} \times 7 \text{ nm}$, $U = -1.2 \text{ V}$, $I = 0.05 \text{ nA}$) of three FePc molecules adsorbed on a monatomic step edge within fcc domains of the reconstructed Au(111) surface. (b) High-resolution STM image ($12 \text{ nm} \times 12 \text{ nm}$, $U = -1.2 \text{ V}$, $I = 0.05 \text{ nA}$) of FePc molecules adsorbed on the reconstructed Au(111) terraces. (c) Line profiles along paths indicated in (a) and (b) revealing the apparent height over the height maximum (dashed black) and along the molecular mirror axis (dashed red) on the step edge, over the two lobes (solid blue) and along the molecular mirror axis (solid green) on the terrace.

image of the molecules on the flat terrace is shown in Figure 3b for comparison. It shows that the FePc molecules are in a flat-lying configuration with D_{4h} symmetry. The line profiles for a flat lying molecule are shown in Figure 3c (solid lines), where the four lobes of the FePc molecule reveal the same height of $\sim 1.75 \text{ \AA}$, while the central iron ion is $\sim 2.0 \text{ \AA}$, which is $\sim 0.25 \text{ \AA}$ higher than the lobes. The maximum heights of both the lobes and the iron ion exist exactly at the central positions, showing a symmetric shape. The left sides of the line profiles appear a little higher than the right sides, which is attributable to the discommensuration lines of the herringbone reconstruction. Comparing

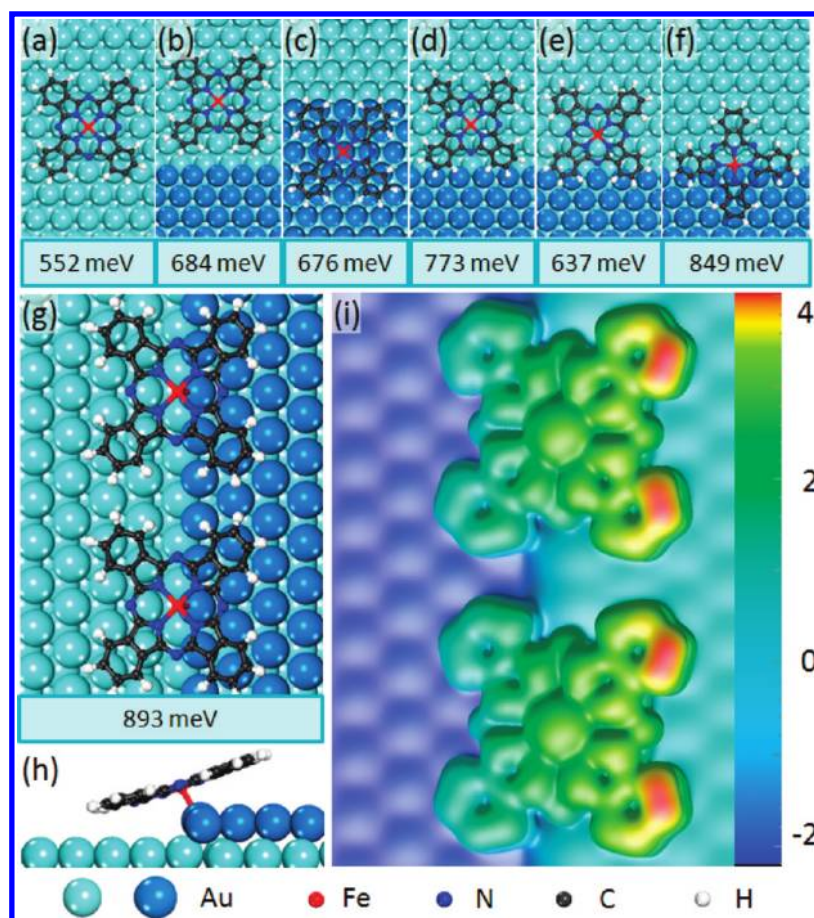


Figure 4. Seven optimized adsorption configurations of FePc molecules on Au(111) surface, where the FePc molecule is located at the (a) free terrace, (b) down terrace, (c) upper terrace, (d) step-edge I, (e) step-edge II, (f) one lobe resting on the upper terrace, (g) top view, and (h) side view of step-edge III. The adsorption energies are provided under each configuration. (i) The calculated STM image of (g) (the STM image is the integrated electron density from -1.2 eV to the Fermi level according to the Tersoff–Hamann approximation^{38,39}). The unit of the calibration bar is in angstroms.

the line profiles of FePc molecules on the step edge to that on a flat terrace, the height increases for the upper lobe, the central iron ion, and the lower lobe are ~ 1.70 , ~ 0.63 , and ~ 0.50 Å, respectively. We know that the STM image is related to the local electron density and the geometric structure. Therefore, where the apparent asymmetric shape of our STM image comes from, a topographical effect or an inhomogeneous distribution of electron, cannot be obtained directly according to the STM image.

To understand the mechanism of selective adsorption of FePc on stepped Au(111) surface and the asymmetric shape of the STM images, a systematic calculation based on DFT is carried out, and the result is discussed in detail as following. Several possible configurations, including the molecules on terrace and on the step edges, are calculated. Because FePc molecules prefer to adsorb on the step located in fcc stacking region (fcc-step-edge) at low coverage, an unreconstructed fcc packing slab model is a good approximation. To compare the influence from the substrate stacking, we also consider one configuration with the FePc molecule adsorbed on the step located in hcp stacking region (hcp-step-edge). For molecules on terraces, unreconstructed fcc packing slab model with four layers of Au(111) is used. For molecules on the steps, two slab models, an unreconstructed fcc packing slab model and an hcp packing slab model, are used to do the calculations. The slab model with steps contains four and a half layers of Au(111) surface to simulate

the step. Figure 4a–c shows three different adsorption sites for molecules on free terrace, down, and up terrace near the monatomic fcc step edge, respectively. The adsorption energies of these configurations are 552, 684, and 676 meV for Figure 4a–c, respectively. For the molecules on the step edge, four adsorption configurations are considered. Three of them are with two lobes resting on the upper terrace near the monatomic fcc step edge (Figure 4d, e, and g); the other one is with only one lobe resting on the upper terrace near the monatomic fcc step edge (Figure 4f). The adsorption energies are 773, 637, 893, and 849 meV for Figure 4d, e, g, and f, respectively.

To investigate the influence from the substrate, a configuration similar to that in Figure 4g, but a slab model with hcp-step-edge, is used. After geometric relaxation, we find that the configurations of molecules on the two steps located in different packing region have similar geometric structures, but with 29 meV energy difference. The adsorption energy of molecules on fcc-step-edge is higher than that on hcp-step-edge, which suggests the molecules prefer to adsorb on fcc-step-edges rather than on hcp-step-edges. We also compare these adsorption energies with that of a molecule on the flat terraces. It is found that the adsorption energy of the molecule on fcc-step-edge is 341 meV higher than that on a terrace. From our DFT calculation results, we can conclude that the fcc-step-edge is the first adsorption site, and the hcp-step-edge site is the second one, then the terraces,

which is in good agreement with the experimental observations. Because of the large difference between the adsorption energy for the FePc molecule on the step edges and that on the free terrace (more than 300 meV), we can obtain a clear STM image only for molecules on the step edges but not for molecules on the terrace at 77 K. Furthermore, the adsorption energy of the configuration with one lobe on the step edge (Figure 4f) is higher than that of the configuration with molecule on flat terrace (Figure 4a), but lower than that with two lobes on the step edge (Figure 4g). It suggests that the configuration in Figure 4f is much more stable than the one with molecule lying flatly on the terrace. This is in good agreement with the experimental observation that the configuration with one lobe on the step edge can be imaged at 77 K, while the molecules on the flat terrace cannot be seen at the same temperature.

To determine the origin of the asymmetric STM image for the configuration with two lobes on fcc-step-edge (Figure 4g), we present the side view of this configuration in Figure 4h. The heights of the lobes (the central iron ion) are the average distances between the carbon atoms (iron atom) on the lobe and the gold atoms on the lower terrace. It is found that the height of the two lower lobes is ~ 3.99 Å, and the height of the central iron ion as well as the two upper lobes is ~ 4.74 and ~ 6.13 Å, respectively. As compared to the corresponding heights in the configuration shown in Figure 4a, the height increases for the lower lobe, the central iron ion, and the upper lobe are ~ 0.75 , ~ 1.70 , and ~ 2.96 Å, respectively. Although these values are slightly larger than the experimental ones, the increasing sequence is in good agreement with experimental results. To find out if this topography fluctuation could induce the asymmetric STM image, STM simulation is done on the basis of the configuration in Figure 4g. Figure 4i shows the simulated STM image for the "on-fcc step edge" configuration,^{38,39} which shows an asymmetric shape. In particular, the simulation reveals the increased heights of the four lobes and the central iron ion of the FePc molecule, which are very close to the experimental observation shown in Figure 3a. Because of its high adsorption energy and the consistent simulated STM image with experimental ones, this specific molecular adsorption configuration and the asymmetrical image is a topographic effect, which results from the FePc molecule leaning on the step edge.

4. CONCLUSIONS

We report on the adsorption behavior of FePc molecules on the reconstructed Au(111) surface with steps by a combination of low temperature STM and DFT calculations. A particularly selective adsorption of FePc molecules on the Au(111) surface with well-controlled adsorption position and molecular orientation is found. The binding energies of FePc on the step edges located in different stacking regions within the $22 \times \sqrt{3}$ reconstructed Au(111) surface are sufficiently different to induce a preferential adsorption of FePc molecules on the fcc step edges. FePc molecules on the monatomic step edge prefer to an asymmetric shape, unlike the symmetric shape of molecules on the flat terrace. The simulated STM image is in good agreement with the experimental observations. These results indicate a promising route for the realization of supramolecular structures, such as molecular chains, based on the well-controlled anchoring of specially designed molecular building blocks on the regularly ordered and stepped Au surfaces.

AUTHOR INFORMATION

Corresponding Author

*Tel.: 0086-10-82648035. Fax: 0086-10-62556598. E-mail: hjgao@iphy.ac.cn (H.-j.G.); sxdu@iphy.ac.cn (S.D.).

ACKNOWLEDGMENT

This work was partially supported by the Natural Science Foundation of China (NSFC), the MOST "973" projects of China, the Chinese Academy of Sciences (CAS), and the Shanghai Supercomputer Center.

REFERENCES

- (1) Crone, B.; Dodabalapur, A.; Lin, Y. Y.; Filas, R. W.; Bao, Z.; LaDuca, A.; Sarpeshkar, R.; Katz, H. E.; Li, W. *Nature (London)* **2000**, *403*, 521.
- (2) Dimitrakopoulos, C. D.; Malenfant, P. R. L. *Adv. Mater.* **2002**, *14*, 99.
- (3) Witte, G.; Wöll, C. *J. Mater. Res.* **2004**, *19*, 1889.
- (4) Horowitz, G. *J. Mater. Res.* **2004**, *19*, 1946.
- (5) Gao, H. J.; Sohlberg, K.; Xue, Z. Q.; Chen, H. Y.; Hou, S. M.; Ma, L. P.; Fang, X. W.; Pang, S. J.; Pennycook, S. J. *Phys. Rev. Lett.* **2000**, *84*, 1780.
- (6) Barlow, S. M.; Raval, R. *Surf. Sci. Rep.* **2003**, *50*, 201.
- (7) Rousset, S.; Repain, V.; Baudot, G.; Garreau, Y.; Lecoeur, J. *J. Phys.: Condens. Matter* **2003**, *15*, S3363.
- (8) Kröger, J.; Jensen, H.; Néel, N.; Berndt, R. *Surf. Sci.* **2007**, *601*, 4180.
- (9) Néel, N.; Kröger, J.; Berndt, R. *Adv. Mater.* **2006**, *18*, 174.
- (10) Yokoyama, T.; Yokoyama, S.; Kamikado, T.; Okuno, Y.; Mashiko, S. *Nature* **2001**, *413*, 619.
- (11) Ruffieux, P.; Palotás, K.; Gröning, O.; Wasserfallen, D.; Müllen, K.; Hofer, W. A.; Gröning, P.; Fasel, R. *J. Am. Chem. Soc.* **2007**, *129*, S007.
- (12) Corso, M.; Auwärter, W.; Muntwiler, M.; Tamai, A.; Greber, T.; Osterwalder, J. *Science* **2004**, *303*, 217.
- (13) Chen, X.; Frank, E. R.; Hamers, R. J. *J. Vac. Sci. Technol., B* **1996**, *14*, 1136.
- (14) Cañas-Ventura, M. E.; Xiao, W. D.; Wasserfallen, D.; Müllen, K.; Brune, H.; Barth, J. V.; Fasel, R. *Angew. Chem., Int. Ed.* **2007**, *46*, 1814.
- (15) Xiao, W. D.; Ruffieux, P.; Ait-Mansour, K.; Gröning, O.; Palotás, K.; Hofer, W. A.; Gröning, P.; Fasel, R. *J. Phys. Chem. B* **2006**, *110*, 21395.
- (16) Craciun, M. F.; Rogge, S.; Morpurgo, A. F. *J. Am. Chem. Soc.* **2005**, *127*, 12210.
- (17) Papageorgiou, N.; Salomon, E.; Angot, T.; Layet, J. M.; Giovannelli, L.; Lay, G. L. *Prog. Surf. Sci.* **2004**, *77*, 139.
- (18) Xing, Lu.; Hipps, K. W.; Wang, X. D.; Mazur, U. *J. Am. Chem. Soc.* **1996**, *118*, 7197.
- (19) Hipps, K. W.; Lu, X.; Wang, X. D.; Mazur, U. *J. Phys. Chem.* **1996**, *100*, 11207.
- (20) Lu, X.; Hipps, K. W. *J. Phys. Chem. B* **1997**, *101*, 5391.
- (21) Barlow, D. E.; Hipps, K. W. *J. Phys. Chem. B* **2000**, *104*, 5993.
- (22) Yoshimoto, S.; Tada, A.; Suto, K.; Itaya, K. *J. Phys. Chem. B* **2003**, *107*, 5836.
- (23) Suto, K.; Yoshimoto, S.; Itaya, K. *J. Am. Chem. Soc.* **2003**, *125*, 14976.
- (24) Yoshimoto, S.; Tsutsumi, E.; Suto, K.; Honda, Y.; Itaya, K. *Chem. Phys.* **2005**, *319*, 147.
- (25) Zhao, A. D.; Li, Q. X.; Chen, L.; Xiang, H. J.; Wang, W. H.; Pan, S.; Wang, B.; Xiao, X. D.; Yang, J. L.; Hou, J. G.; Zhu, Q. S. *Science* **2005**, *309*, 1542.
- (26) Gao, L.; Liu, Q.; Zhang, Y. Y.; Jiang, N.; Zhang, H. G.; Cheng, Z. H.; Qiu, W. F.; Du, S. X.; Liu, Y. Q.; Hofer, W. A.; Gao, H. J. *Phys. Rev. Lett.* **2008**, *101*, 197209.

- (27) Gao, L.; Deng, Z. T.; Ji, W.; Lin, X.; Cheng, Z. H.; He, X. B.; Shi, D. X.; Gao, H. J. *Phys. Rev. B* **2006**, *73*, 075424.
- (28) Wang, Y. L.; Ji, W.; Shi, D. X.; Du, S. X.; Seidel, C.; Ma, Y. G.; Gao, H. J.; Chi, L. F.; Fuchs, H. *Phys. Rev. B* **2004**, *69*, 075408.
- (29) Seidel, C.; Poppensieker, J.; Fuchs, H. *Surf. Sci.* **1998**, *408*, 223.
- (30) Vanderbilt, D. *Phys. Rev. B* **1990**, *41*, 7892.
- (31) Kresse, G.; Furthmüller, J. *Phys. Rev. B* **1996**, *54*, 11169.
- (32) Perdew, J. P.; Burke, K.; Ernzerhof, M. *Phys. Rev. Lett.* **1996**, *77*, 3865.
- (33) Harten, U.; Lahee, A. M.; Toennies, J. P.; Wöll, Ch. *Phys. Rev. Lett.* **1985**, *54*, 2619.
- (34) Wöll, Ch.; Chiang, S.; Wilson, R. J.; Lippel, P. H. *Phys. Rev. B* **1989**, *39*, 7988.
- (35) Barth, J. V.; Brune, H.; Ertl, G.; Behm, R. J. *Phys. Rev. B* **1990**, *42*, 9307.
- (36) Cheng, Z. H.; Gao, L.; Deng, Z. T.; Liu, Q.; Jiang, N.; Lin, X.; He, X. B.; Du, S. X.; Gao, H. J. *J. Phys. Chem. C* **2007**, *111*, 2656.
- (37) Cheng, Z. H.; Gao, L.; Deng, Z. T.; Jiang, N.; Liu, Q.; Shi, D. X.; Du, S. X.; Guo, H. M.; Gao, H. J. *J. Phys. Chem. C* **2007**, *111*, 9240.
- (38) Tersoff, J.; Hamann, D. *Phys. Rev. B* **1985**, *31*, 805.
- (39) Tersoff, J.; Hamann, D. *Phys. Rev. Lett.* **1983**, *50*, 1998.